Image Processing Techniques for Space Situational Awareness

Performing Photometry on James Webb Space Telescope Imagery from NEOSSat

Michael Ian Stewart
York University, Toronto Canada
Dr. Regina Lee
York University, Toronto Canada

Shane Ryall
Defence Research and Development Canada

ABSTRACT

Space Situational Awareness (SSA) is paramount for monitoring and managing the expanding population of space objects, encompassing active satellites, debris, and potential threats, collectively known as Resident Space Objects (RSOs). Image processing techniques have emerged as invaluable tools for bolstering SSA capabilities, offering critical insights into space object detection, tracking, and characterization. This study addresses a significant research gap by focusing on the measurement of cis-lunar RSOs utilizing space-based sensors. Leveraging the capabilities of the Defense Research and Development Canada (DRDC) research satellite NEOSSat, this research conducted observations of the James Webb Space Telescope (JWST). An innovative image processing pipeline was developed to accommodate JWST's unique Earth-Sun L2 Orbit and overcome NEOSSat's challenges, including a high noise floor, uneven temperature regulation, and the inability to reliably capture dark frames. The resulting calibrated photometric light curve exhibits distinctive patterns, which are hypothesized to be attributed to NEOSSat's right ascension and the relative distances between RSOs. This study advances our understanding of SSA methodologies and contributes to the evolving field of space object monitoring.

1. INTRODUCTION

Resident Space Objects (RSOs), encompassing artificial satellites and associated debris orbiting Earth, constitute a vital component of our modern technological infrastructure. Ensuring their precise monitoring, understanding, and prediction falls under the realm of Space Situational Awareness (SSA). Accurate tracking of RSOs is essential for gathering valuable data to unravel their mysteries. The James Webb Space Telescope (JWST) presents an intriguing case study for experimenting with innovative image processing techniques. Its publicly available observation catalog, substantial size, and unique orbit at the Sun-Earth L2 point render it an exceptional target for exploration. However, the distinctive characteristics that make JWST an enticing subject also necessitate a departure from traditional SSA image processing pipelines. To observe JWST, we employed the space-based sensor NEOSSat, offering unobstructed views unaffected by atmospheric turbulence. Nevertheless, NEOSSat comes with its own set of challenges, including suboptimal temperature regulation and high noise levels, mandating an image processing approach distinct from typical ground-based sensors. This paper details the development of an image processing pipeline tailored to images of JWST captured by NEOSSat during one half-period of NEOSSat's orbit. The pipeline commences with RSO location prediction, progresses through image reduction, and culminates in photometry. Our choice of observation time aligns with JWST's lock on the star TOI-836, ensuring that the resulting light curve reflects the unique characteristics of the NEOSSat satellite itself.

2. DATA ACQUISITION

2.1 Tracking

Many Resident Space Objects (RSOs) can be characterized by Two Line Element (TLE) Sets containing mean orbital elements. Utilizing a Simplified General Perturbation model (SGP4) [4], we propagated the target RSOs forward or

backward in time to align with our desired observation epoch. However, an inherent challenge emerged when dealing with RSOs that defy TLE approximation, such as the James Webb Space Telescope (JWST) situated at the Sun-Earth L_2 Lagrange point.

To surmount these obstacles, we harnessed the *astroquery* package [6], which provided access to ephemerides via the JPL Horizons online API. This enabled us to obtain precise position and velocity information for non-TLE compliant RSOs like JWST. However, the JPL Horizons API is built mainly for ground-based observatories and only allows for querying objects from longitude, latitude and altitude as the observer. As our data was acquired via the space-based NEOSSat sensor, we required NEOSSat's state vector to be converted to longitude, latitude, and altitude as input for JPL Horizons. Conversion between state vector and longitude latitude and altitude was implemented differently depending on whether a TLE or state vector was used. This approach allowed us to obtain accurate ephemerides and positional information necessary for our observations, enabling precise data analysis.

NEOSSat tracking involved two distinct modes: an initial prediction phase for determining NEOSSat's pointing direction and a post-acquisition prediction phase used to locate the James Webb Space Telescope (JWST) within NEOSSat-captured images. Figure 1 illustrates the image processing pathways employed for both the initial prediction and post-acquisition prediction phases.

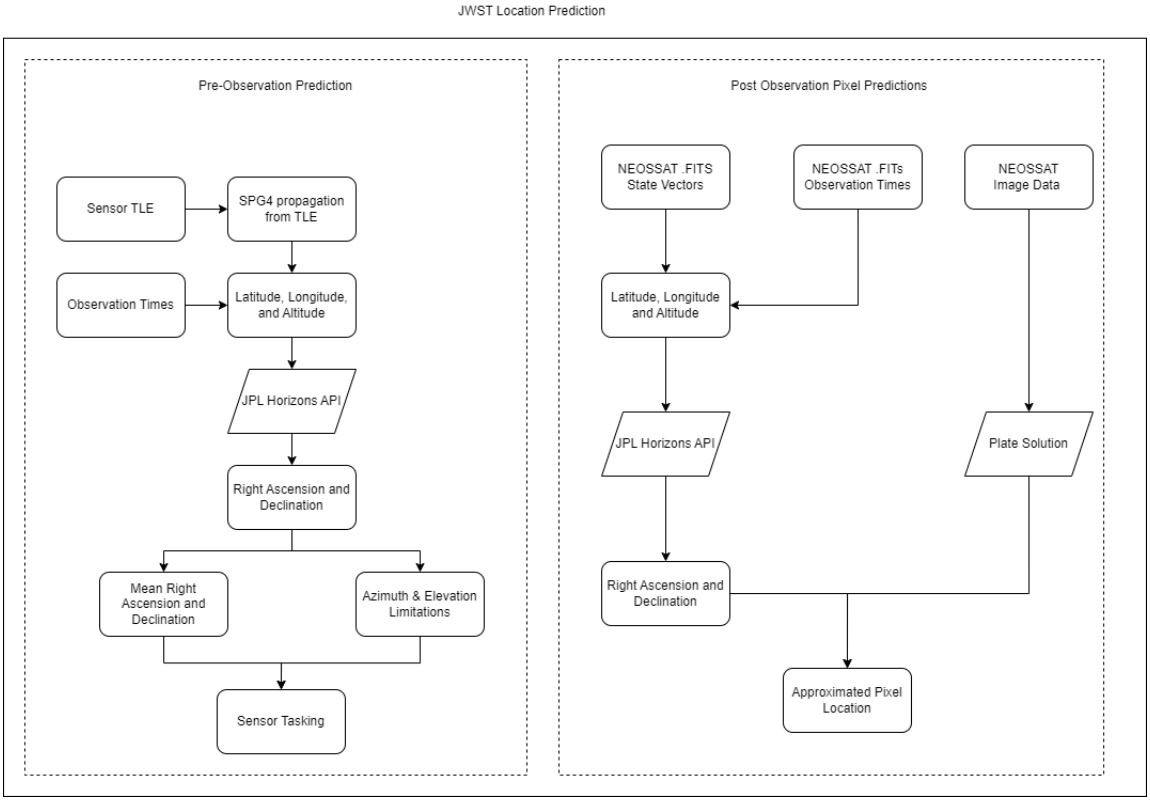

Fig. 1: Estimating the position of JWST

2.1.1 Initial Prediction

For the chosen date of March 08 2023, the up-to-date epoch TLE for NEOSSat was obtained from Celestrak.org and redefined in a visualization script using Brandon Rhode's *skyfield* [7]. The satellite object was then cast to latitude, longitude and altitude using a WGS84 ellipsoid at a multitude of epochs. After the JPL Horizon is queried using the longitude latitude and altitude the the right ascension and declination are outputted. A Digitized Sky Survey (DDS) image was generated using AstroPy's *astropan* to cover the extent of the right ascensions and declination generated.

The World Coordinate System (WCS) information from the generated image is used to 'draw' the pixel locations of the right ascension and declination creating Figure 2. One orbit of NEOSSat is seen on the right image of Figure 2 when the epochs are restricted to a 105 minute spread.

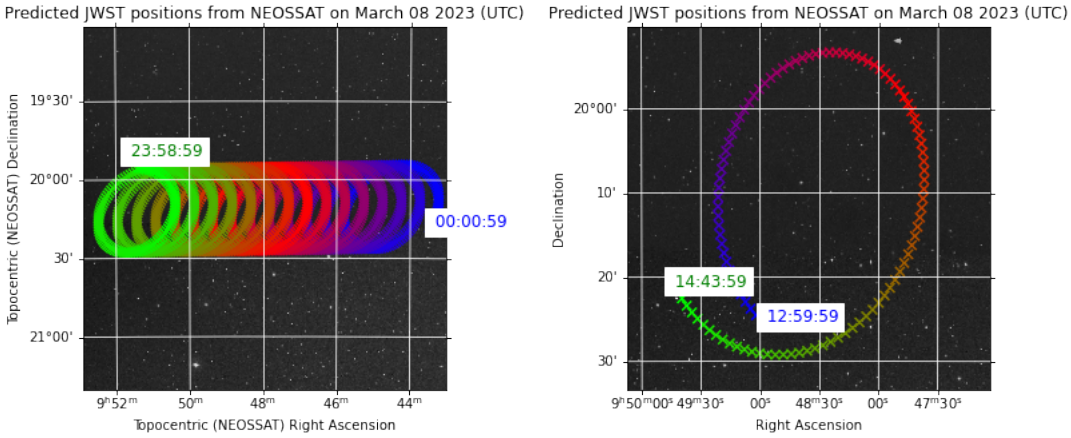

Fig. 2: Predicted location of JWST with DSS background

The path that JWST takes when viewed from NEOSSat follows an elliptical patter. The circular shape shifts slightly with each rotation and NEOSSat is adjusted to compensate every orbit (1 orbit being 105 minutes). NEOSSat was aimed at the middle of the circular pattern for several reasons: image processing would be simplified with star matching and NEOSSat cannot accurately track RSOs with small mean motion (relative to other RSOs).

The ideal predicted location presented in Figure 2 is not representative of NEOSSat's orbit as the sensor will move behind the Earth, obstructing the view to JWST. In order to model restrictions of NEOSSat's look angles, the satellite is mimicked as a ground-based station. The ground-based 'topocetric horizon' look angles (Azimuth and Elevation) are calculated along with the right ascension and declination and an elevation restriction of 0 degrees is applied to the prediction location data resulting in Figure 3.

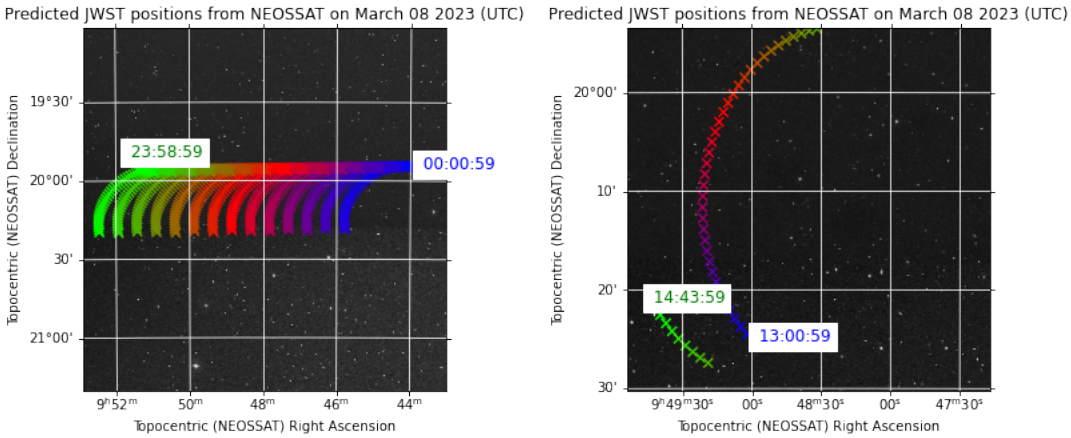

Fig. 3: Estimated locations of the JWST as seen from NEOSSat with elevation restrictions

2.2 Post-Acquisition Prediction

The predicted locations of JWST were used to direct the sensor and capture a series of 100 images per orbit for several orbits. Data captured on March 08 2023 was used for this case study. The images captured contained accurate values for cartesian state vectors and the latitude and longitude of NEOSSat saved in the image's .FITs headers. The state

vector was used to predict the height above the WGS84 ellipsoid which was then used jointly with the measurements of latitude and longitude as inputs for Horizon's API. On March 08th 2023, the following predicted locations were produced in Figure 4.

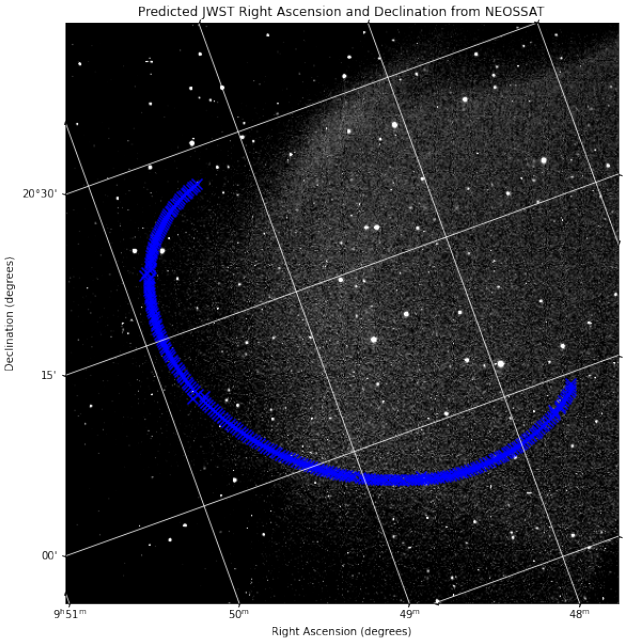

Fig. 4: Predicted locations of JWST displayed on a background star field on March 08 2023

3. IMAGE REDUCTION

The astronomer's approach to reducing astronomical images includes the use of flat frames, bias frames and dark frames. With NEOSSat being a space-based sensor, capturing Flat frames could not be achieved. Similarly, the mechanical shutter of NEOSSat could only be closed once after each orbit limiting the ability to capture dark frames. Bias and pseudo-dark frames are captured during the observation sequence in order to reduce the images. In each 105-minute orbit described in Section 2.1, 100 light images were captured along with 5 bias frames and 10 pseudo-dark frames.

Figure 5 describes the image reduction workflow for images captured by NEOSSat.

3.1 Overscan and Fourier Deconvolution

The overscan region, extending beyond the main imaging area on a sensor, captures baseline electrons generated by pixels without photon introduction. Its location is recorded in .FITS headers, and the average is calculated within specified bounds. NEOSSat noise floor, seen in the overscan region is describable through Fourier transform. The amplitude and frequency of an overscan region is measured using a fast fourier transform (FFT) and a 3 sigma cutoff mask is applied to the image. The overscan's Fourier model is then subtracted from the background of the non-masked data.Once the overscan region value is averaged and a fourier model is constructed, the overscan is trimmed from each image so that negative values are not present in the image when it is reduced further.

3.2 Bias Frames

Bias frames, also known as zero frames, are essential components of the image reduction process. They are images captured with zero exposure time, solely registering the electronic noise and offset levels inherent to the image sensor. These frames are critical for quantifying and correcting electronic noise, including readout noise, that can introduce variations in pixel values. Bias frames are overscan subtracted and trimmed, then combined and subtracted from all other frames resulting in cleaner and more accurate images.

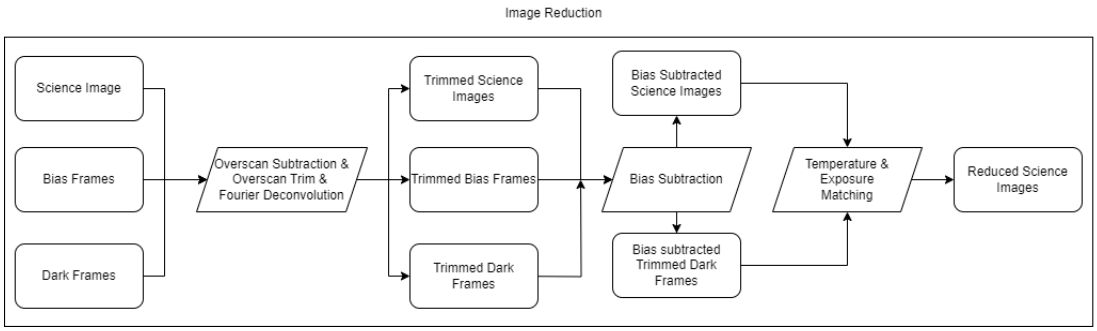

Fig. 5: Reduction flow of NEOSSat images

3.3 Dark Frames

NEOSSat's sensor can only use its mechanical shutter at the end of each orbit, thus eliminating the capability to produce traditional dark frames in a convenient manner. A workaround for this issue is to capture frames of the same exposure time and temperature as the science frames during the desaturation of the NEOSSat's momentum wheels. During the capture of these pseudo-dark frames, the sensor is rotating rapidly, meaning that each image that is captured contains different light sources. When a master dark is created, the light sources are averaged out and the resulting image appears to be a 'close-enough' approximation to a traditional master dark. Due to the lack of perfect temperature regulation on NEOSSat, the temperatures of the dark frames have to be matched to the science frames in order to reduce the frames properly. The approach taken in this study matched five dark frames according to the temperature and exposure of the light frame, then created a master dark from those files. The master bias is then subtracted from the master darks and the science frames creating a reduced science image.

3.4 Science Frames

A science frame is a captured image intended to record astronomical data. Unlike calibration frames, which correct for technical factors like sensor biases, dark currents, and flat-fielding, a science frame captures the actual light or emissions from celestial objects. JWST science frames are reduced with the bias and dark frames then photometric methods are used to measure the light received from the target and surrounding stars. The surrounding stars are compared with their catalogue values to calibrate the produced light curve.

4. PHOTOMETRY

Performing photometry on reduced light/science frames involves several general steps. Firstly the background must be estimated, secondly the light sources detected, and thirdly these sources must be identified and matched up to their catalogue values. Figure 6 defines the flowchart used to perform photometry on a reduced dataset. The first image of each data can be used to approximate the zeropoints of the dataset, the aperture radius for aperture photometry, as well as the aperture corrections required for calculating instrumental magnitude.

4.1 Background Estimation

After reduction, the background of each reduced science frame has to be calculated. This was implemented with the help of AstroPy [1] [2] [3]. In specific, a Python implementation of the SExtractor algorithm [5] was used to estimate the background. The background was subsequently subtracted from the reduced science image resulting in an image where light source could be easily detected if their values were about 0 Analog Digital Units (ADU).

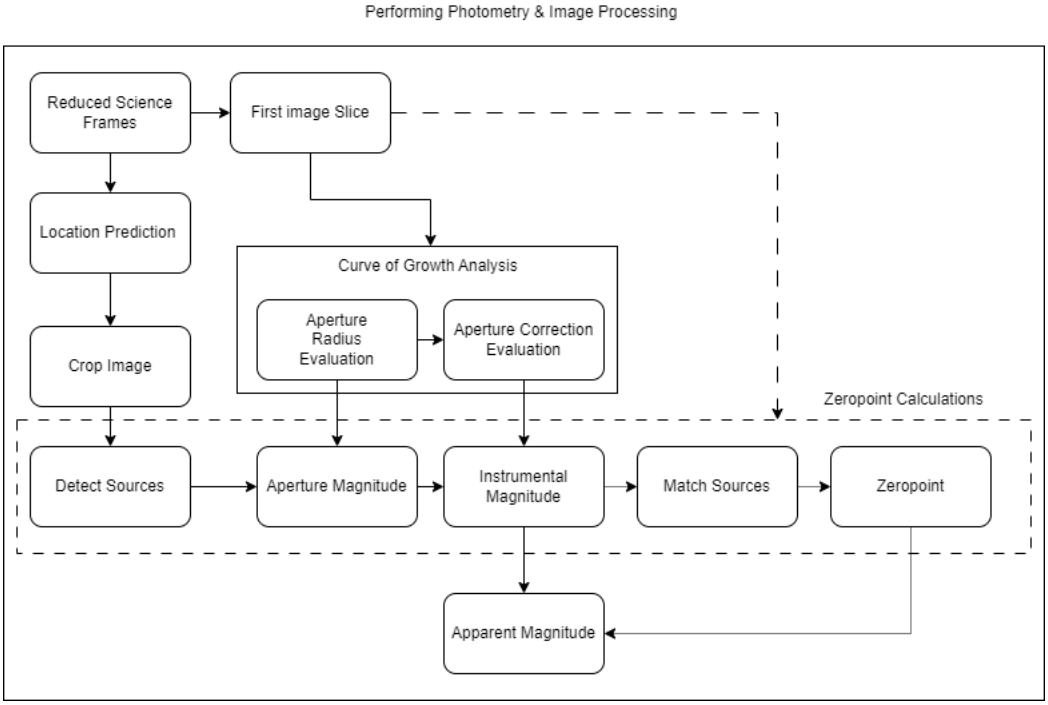

Fig. 6: JWST-NEOSSat photometry process

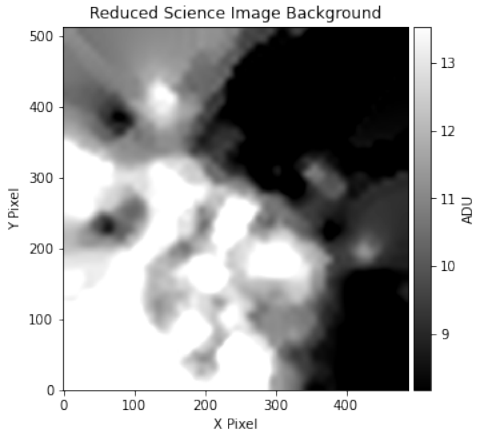

Fig. 7: The background estimated in a reduced image

4.1.1 Light Source Detection

Three methods light source detection methods were looked at to determine their viability; the *detect_sources* method, *Source Extractor for Python (SEP)* and *IRAF starfind*. A comparison of these methods is shown in Table 1. The detected sources were matched against a the Fourth U.S. Naval Observatory CCD Astrograph Catalogue (UCAC4) catalogue to determine the detection rates.

AstroPy's *detect_sources* along with the *Source Catalog* function proved to be the most useful method for detecting the sources due to its lack of reliance on a pre-known point spread function (PSF), its versatility, and match accuracy.

Results	SEP	SourceCatalog	IRAF
Number of Matched Sources	343	312	254
Match Accuracy (Out of 100)	97.72	97.81	92.36

Table 1: Statistics of the matched stars with catalogue stars

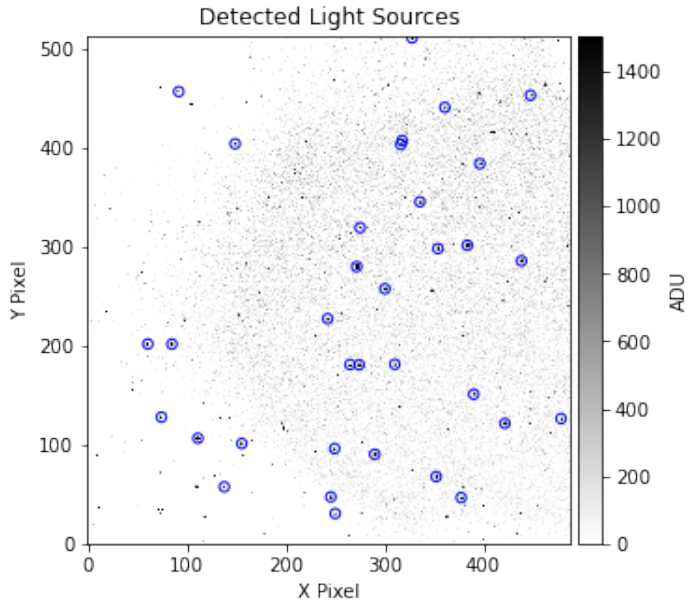

Fig. 8: Detected sources with AstroPy's detect_sources method marked with blue circles

4.2 Aperture Photometry

The chosen approach for conducting photometry on the acquired data involved using aperture photometry. This technique encompasses several steps: selecting the aperture, measuring the flux, performing aperture correction, which leads to the determination of an instrumental magnitude. Afterwards, the instrumental magnitudes of the detected sources were cross-referenced with a star catalogue, enabling the calculation of a zeropoint for the conversion of instrumental magnitudes to apparent magnitudes.

4.2.1 Choosing an Aperture

To determine the optimal aperture for aperture photometry, an assessment of the signal-to-noise ratio of stars within the image was conducted. Within this dataset, the five brightest stars were selected to establish the most suitable aperture radius, ensuring uniformity across the entire image and dataset. Figure 9 displays the signal-to-noise ratios of the five brightest stars used to determine the appropriate radius for aperture photometry.

4.2.2 Aperture Magnitude Offset

When aperture photometry is performed additional information from the light source is 'cut off'. For this reason, a magnitude offset needs to be calculated to compensate for this information loss. The magnitude offset is calculated from the aperture magnitude at the best aperture radius and the asymptotic magnitude. Figure 10 shows the calculated aperture corrections in red and their relation to the aperture magnitude and asymptotic magnitude.

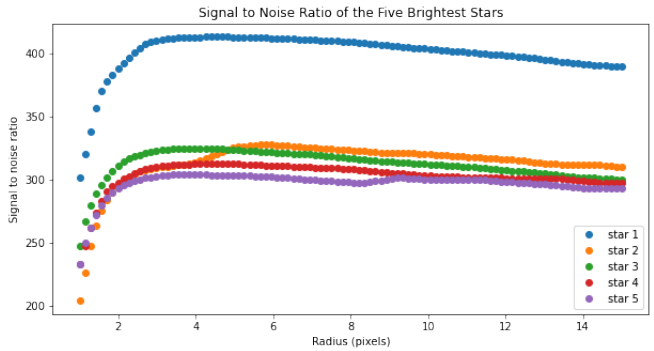

Fig. 9: The signal-to-noise ratio of the five brightest stars

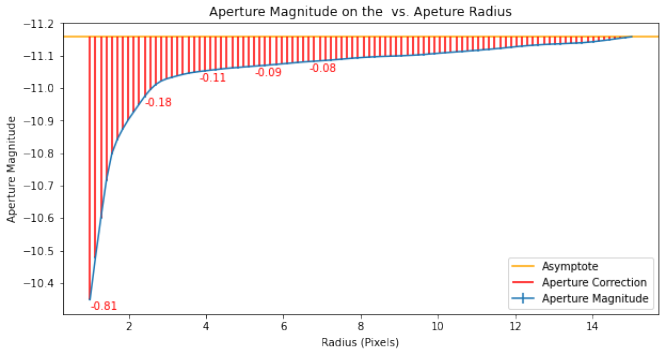

Fig. 10: Aperture correction from the five brightest stars in the image

4.3 Plate Solution

Part of the location prediction problem was resolving a plate solution from each image. A plate solution matches the pixel locations of stars in an image to celestial coordinates. The output World Coordinate System (WCS) information from a plate solution acts as a map to directly convert each pixel to right ascension and declination. Visual Pinpoint was used to plate solve each image in the dataset as plate solutions could be obtained in several milliseconds.

4.4 Star Matching

$$V = v - Zp$$

- V: visual magnitude
- v: instrumental magnitude
- Zp: Zeropoint

With the reduced dataset plate-solved, the stars in each image are matched to their respective catalogue values. The instrumental magnitudes of the stars were then aligned with the Visual Magnitude (VMag) values from UCAC4 to establish a precise zero-point value.

4.5 Locating JWST In An Image

4.5.1 Cropping

To increase the speed of which images are processed, a 10 by 10 square crop around the expected location of JWST was was made. Sources are then detected within this crop and subsequently mapped back onto the original image. The

data is cropped using the *Cutout2D* function provided by AstroPy.

4.5.2 Proximity Correlation

The Right Ascension and Declination found by the JPL Horizon's API is converted to pixel locations with the use of the plate solution WCS information. These pixel coordinates are then proximity correlated to the detected sources. The detected sources that are closest to the estimated pixel locations are tagged as the source of interest.

5. RESULTS

With the appropriate aperture radius chosen from Figure 9, aperture correction from Figure 10, and predicted locations from Figure 4 the aperture and instrumental magnitudes of JWST are extracted resulting in Figure 11.

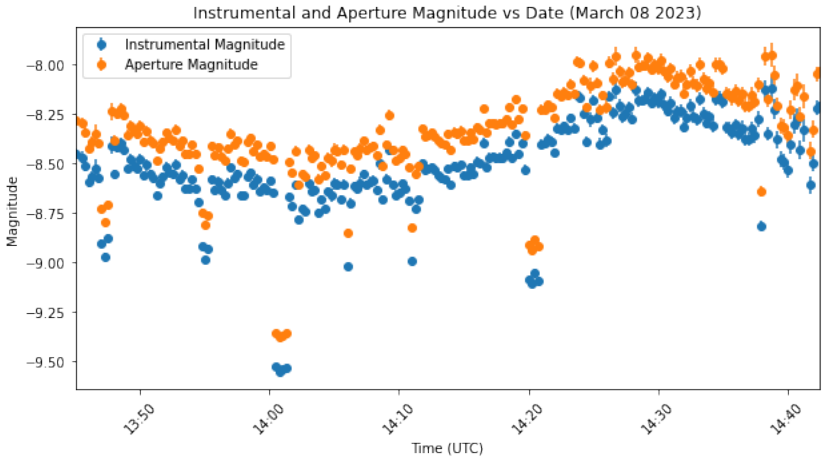

Fig. 11: Instrumental and aperture magnitudes of JWST vs. time

In the background of all the images, stars are detected stars and with the aperture radius calculated in Figure 9, the instrumental magnitude of the brightest 20 stars are extracted. Comparing the detected stars to their catalogue values, results in zeropoint values in Figure 12. Applying the zeropoints to the instrumental magnitudes of JWST seen in

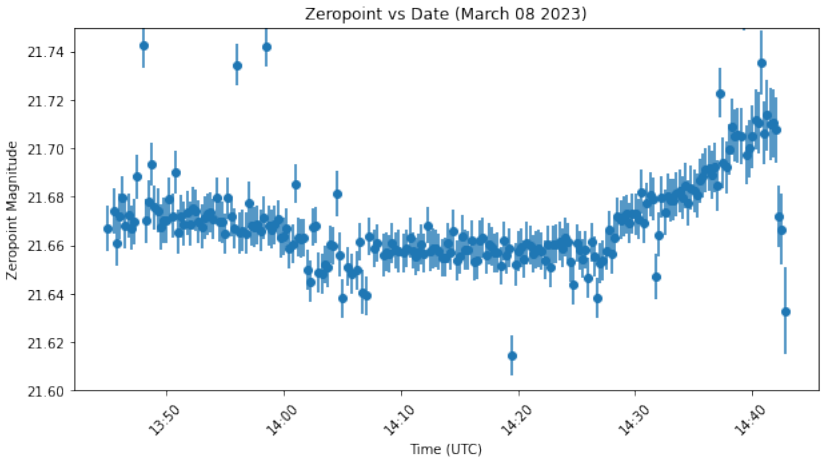

Fig. 12: The calculated zeropoints from the stars in the image vs. time

Figure 11 gives apparent magnitudes seen in Figure 13.

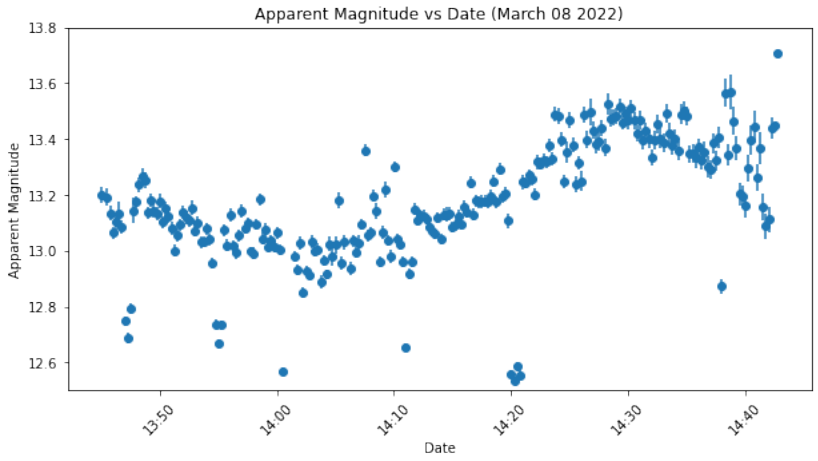

Fig. 13: The calculated apparent magnitude vs. time on March 08 2023

Comparing the estimated centroids of JWST against it's measured centroids produced Figure 14.

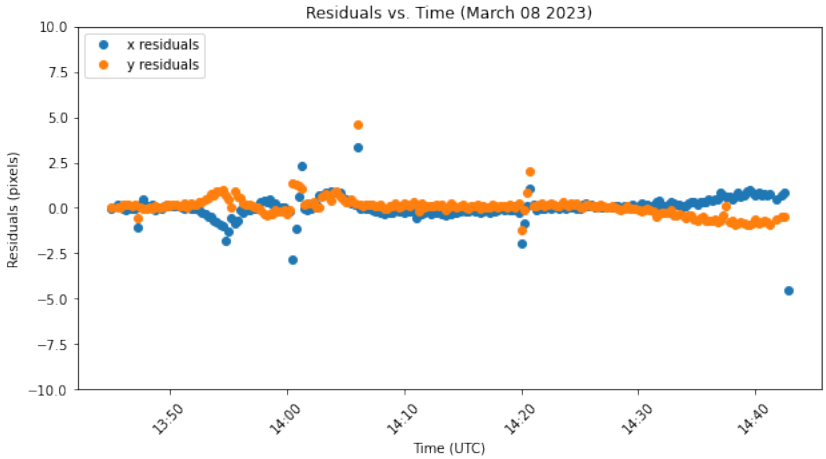

Fig. 14: Residuals between estimated x and y centroid locations and measured centroids

5.1 Schedule Matching

With JWST being an internationally-used scientific instrument, the observing schedule for JWST is publicly available. Downloading the weekly schedules pertaining to the satellite, they can be compared against the light curve to determine any shifts in the signal received. The schedules can be found at the Space Telescope Science Institute [8]. Matching the observations of JWST with the schedule shows that JWST was looking at **TOI-836** during the entire sample dataset presented in this paper. JWST's lock on **TOI-836** ensures that there are minimal changes in specular reflectivity between the frames.

6. DISCUSSION

The process for identifying JWST in images captured by NEOSSat proves to be effective. By using a simple proximity correlation to estimated positions, JWST was identified accurately more than 97% of the time. Conjunctions with stars in the images created rapid spike or dips in light. Despite flux outliers being troublesome they can be filtered out in post-processing when analysing either Figure 14 or Figure 13. Caution will need to be taken for each processed image dataset to ensure the residuals do not drift from less than 5 pixels, such is the case when an RSO is not measured correctly or propagated with the most up to date TLE. The produced light curve, seen in Figure 13, shows minimal variations besides the expected sinusoidal wave resulting from the instrumental magnitude. It should be noted for further photometric analysis with space-based sensors that the observing satellite's orbit may affect the resulting light curve and that measurement should also be normalized by distance. Further investigation will need to be conducted on a larger dataset to attempt to associate changes in light curve spikes with changes in the observed targets by JWST and how severely the orbital parameters affect the flux received by the sensor.

7. CONCLUSIONS

The methods described in this paper proved to be effective in performing photometry on JWST with NEOSSat. Working around the restrictions of the observed and observing RSO, the created script produced a stable light curve that reflects the distance to the target and orbit of NEOSSat. Further research will need to be conducted on a larger set of data to analysis other patterns that could be present with such sensors.

REFERENCES

[1] Astropy Collaboration and Astropy Contributors. Astropy: A community Python package for astronomy. , 558:A33, October 2013.

[2] Astropy Collaboration and Astropy Contributors. The Astropy Project: Building an Open-science Project and Status of the v2.0 Core Package. , 156(3):123, September 2018.

[3] Astropy Collaboration and Astropy Project Contributors. The Astropy Project: Sustaining and Growing a Community-oriented Open-source Project and the Latest Major Release (v5.0) of the Core Package. *apj*, 935(2):167, aug 2022.

[4] Roger R. Bate, Donald D. Mueller, and Jerry E. White. *Fundamentals of Astrodynamics*. Dover Publications, New York, 1971.

[5] E. Bertin and S. Arnouts. SExtractor: Software for source extraction. , 117:393–404, June 1996.

[6] Michael Mommert, Michael S. p. Kelley, Miguel de Val-Borro, Jian-Yang Li, Giannina Guzman, Brigitta Sipőcz, Josef Ďurech, Mikael Granvik, Will Grundy, Nick Moskovitz, Antti Penttilä, and Nalin Samarasinha. sbpy: A python module for small-body planetary astronomy. *Journal of Open Source Software*, 4(38):1426, 2019.

[7] Brandon Rhodes. Skyfield: High precision research-grade positions for planets and Earth satellites generator. Astrophysics Source Code Library, record ascl:1907.024, July 2019.

[8] STSci. James webb space telescope (jwst) science execution: Observing schedules. `https://www.stsci.edu/jwst/science-execution/observing-schedules`, 2023. Accessed on August 1, 2023.